Article

Effect of Fluorescently Labeling Protein Probes on Kinetics of Protein#Ligand Reactions

Y. S. Sun, J. P. Landry, Y. Y. Fei, and X. D. ZhuJ. T. Luo, X. B. Wang, and K. S. Lam

Langmuir, **2008**, 24 (23), 13399-13405 • Publication Date (Web): 08 November 2008

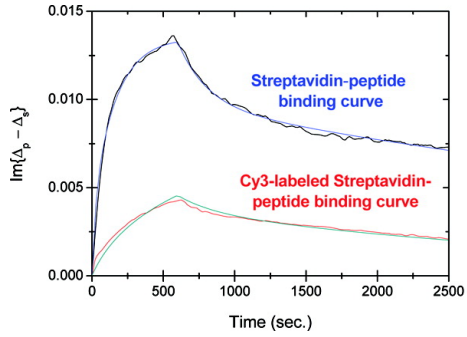

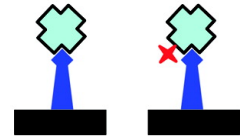

More About This Article

Additional resources and features associated with this article are available within the HTML version:

- Supporting Information
- Access to high resolution figures
- Links to articles and content related to this article
- Copyright permission to reproduce figures and/or text from this article

View the Full Text HTML

Effect of Fluorescently Labeling Protein Probes on Kinetics of Protein−Ligand Reactions

Y. S. Sun, J. P. Landry, Y. Y. Fei, and X. D. Zhu*

Department of Physics, University of California, Davis, California 95616

J. T. Luo, X. B. Wang, and K. S. Lam

School of Medicine, University of California at Davis, Sacramento, California 95817

Received July 7, 2008. Revised Manuscript Received September 24, 2008

We studied the effect of fluorescently labeling proteins on protein−ligand reactions. Unlabeled ligands (*streptavidin-binding* peptides and rabbit immunoglobulin G (IgG) as antigen targets) are immobilized on epoxy-functionalized glass slides. Unlabeled and Cy3-labeled protein probes from the same batch (streptavidin and goat antibodies) subsequently react with the surface-immobilized targets. By monitoring *in situ* the surface mass density change using an oblique-incidence reflectivity difference scanning microscope (a label-free detector), we measured k_{on} and k_{off} for streptavidin−peptide reactions and antibody−antigen reaction. We found that (1) equilibrium dissociation constants, defined as $K_D = k_{off}/k_{on}$, for streptavidin−peptide reactions increases by a factor of 3−4 when the solution-phase streptavidin is labeled with Cy3 dye and (2) K_D for reactions of solution-phase goat anti-rabbit antibodies with rabbit IgG targets also change significantly when the goat antibodies are labeled with Cy3 dye.

1. Introduction

Biomolecular processes are commonly characterized and quantified to an extent by fluorescence-based detection methods.[1−4] Fluorescence-based detection is preferred for high sensitivity, safety, and relative ease of use and for an increasingly large selection (in physiochemical/structural properties and biocompatibility) of labeling agents including fluorophores, green fluorescence protein, phytochrome proteins, semiconductor quantum dots, metal cages, and others.

However, it is known that labeling either the protein or its ligand with extrinsic fluorescent molecules for purposes of detection may change innate characteristics of protein−ligand interaction and subsequent biochemistry involving the ligand, the protein, or their complex.[3,4] Fluorescently labeling deoxynucleotide triphosphates (dNTPs) is known to reduce the rate of incorporation (with high fidelity polymerases) by more than 1 order of magnitude and limits the total length of primer extension due to stereochemical hindrance.[5] Impairment or degradation of original protein functions is an often encountered effect of fluorescence labeling. The potential to enact new functions by a fluorescent labeling agent can be a blessing as well as undesirable, given the multifunctionality of a protein (e.g., Met protein[6]). However, how a fluorescent tag quantitatively changes the affinity of a protein to its ligands is generally lesser known, mainly due to lack of experiments that directly compare the binding affinity of a native protein with a native ligand with the affinities obtained when either the protein or the ligand is fluorescently labeled under the same reaction condition. Such information is important in evaluating the benefit, reliability, and risk of using fluorescence-based detections for specific studies of biomolecular processes. In this paper, we take a step toward addressing this issue. Specifically, we report a set of experimental studies of the effect of fluorescently labeling proteins on binding constants of protein−ligand reactions.

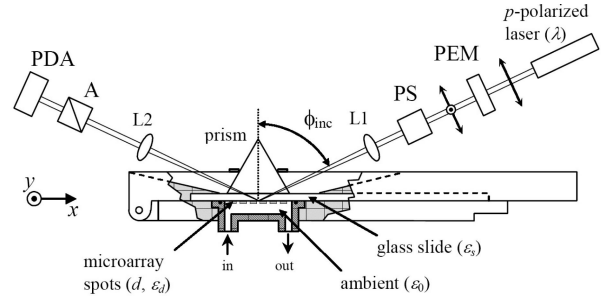

Figure 1. Sketch of an oblique-incidence reflectivity difference (OI-RD) scanning microscope for detection of association and dissociation of solution-phase protein with ligand microarrays immobilized on a glass slide surface. It employs the total internal reflection geometry for illumination and a combination of a 152-element photodiode array (PDA) for the *y*-scan and a mechanical translation stage for the *x*-scan. PEM, photoelastic modulator that changes the polarization of the illumination laser beam at 50 kHz; PS, variable phase-shifter; L1, cylindrical lens that focuses the illumination laser beam to a line segment on the sample surface; L2, 10× objective lens that forms an enlarged image of the illuminated line segment across the PDA; A, polarization analyzer.

2. Materials and Methods

Protein Probes. Cy3-labeled and unlabeled streptavidin tetramers were purchased from Jackson ImmunoResearch Laboratories (West Grove, PA) and used without further purification. According the manufacturer, Cy3 molecules were conjugated to streptavidin through reaction of Cy3 Bis NHS ester with primary amines on lysine residuals on the protein. The Cy3-to-streptavidin ratio is 2.5−3.5 according to the manufacturer's specification. It is noteworthy that one streptavidin tetramer has a total of 16 primary amines. Cy3-labeled and unlabeled monovalent F_{ab} fragments (∼50 kDa) of goat immunoglobulin G (IgG) against the (H+L) domain of rabbit IgG

* To whom correspondence should be addressed. E-mail: xdzhu@physics.ucdavis.edu.

(1) Schena, M. *Microarray Analysis*; John Wiley and Sons: Hoboken, NJ, 2003.
(2) Zhu, H.; Bilgin, M.; Bangham, R.; Hall, D.; Casamayor, A.; Bertone, P.; Lan, N.; Jansen, R.; Bidlingmaier, S.; Moufek, T.; Mitchell, T.; Miller, P.; Dean, R. A.; Gerstein, M.; Snyder, M. *Science* **2001**, *293*, 2101–2105.
(3) MacBeath, G. *Nat. Genet.* **2002**, *32*, 526–532.
(4) Kodadek, T. *Chem. Biol.* **2001**, *8*, 105–115.
(5) Quake, S. Private communication.
(6) Jarvis, L. M. *Chem. Eng. News* **2007**, *85*, 15–23.

10.1021/la802097z CCC: $40.75
Published on Web 11/08/2008

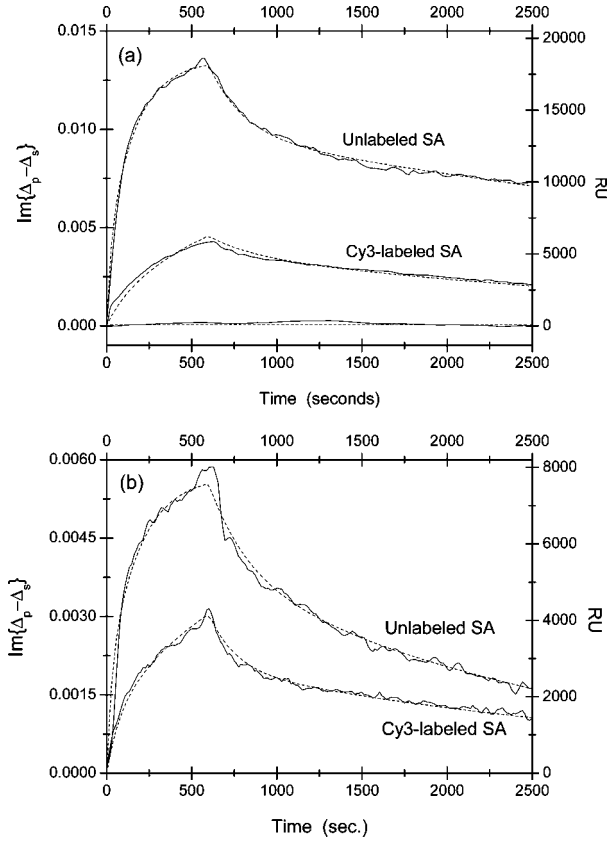

Figure 2. Real-time association−dissociation curves of solution-phase streptavidin (SA) with immobilized peptide−BSA conjugates on an epoxy-coated glass slide. The concentration of streptavidin is 1 μM in both measurements. (a) Reactions of streptavidin with *linear SAWSHPQFEK*-BSA conjugates. The curve near zero is the association−dissociation curve of streptavidin with a BSA control spot, which shows no evidence of nonspecific reaction between BSA and streptavidin. (b) Reactions of streptavidin with disulfide-bridged *cyclic CHPQGPPC*−BSA. The optical signal $\mathrm{Im}\{\Delta_p - \Delta_s\}$ is related to the captured streptavidin through eqs 2 and 4b.

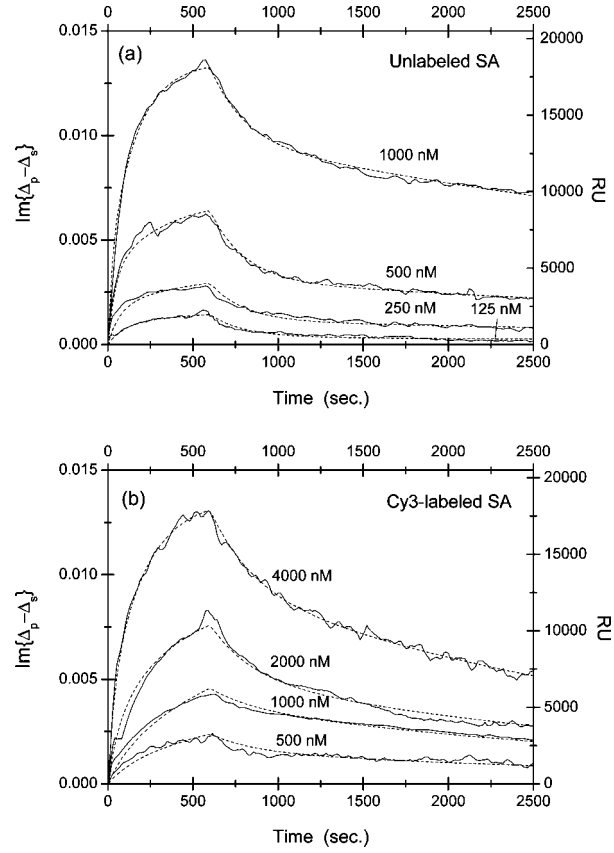

Figure 3. Association−dissociation curves of (a) unlabeled and (b) Cy3-labeled streptavidin with surface-immobilized *linear SAWSHPQFEK*−BSA conjugates at different streptavidin concentrations. It should be noted that the probe concentrations in (b) are 4 times larger than those in (a). The curves are globally fitted (dotted lines) to a two-site Langmuir reaction model (see main text for details) with the global fitting parameters listed in Table 1.

were also purchased from Jackson ImmunoResearch Laboratories. By request, the Cy3-labeled and unlabeled monovalent F_{ab} fragments were from the same batch. The Cy3-to-monovalent F_{ab} fragment ratio is 2.5−3.5. Cy3-labeled and unlabeled goat whole IgG against the F_c domain of rabbit IgG from the same batch were also purchased from Jackson ImmunoResearch Laboratories as well. The Cy3-to-F_c fragment ratio is 4−6.

Ligand and Protein Targets. Unlabeled affinity-purified rabbit IgG as targets for goat anti-rabbit IgG was purchased from Jackson ImmunoResearch Laboratories (West Grove, PA). We synthesized two Aoa (aminooxyacetic acid)-linked peptides, disulfide-bridged *cyclic CHPQGPPC* and linear *SAWSHPQFEK*, as targets for streptavidin.[7] The *HPQ* domain on these two peptides is known to be the motif that binds to the biotin-binding pocket on streptavidin.[8−11] The crystal structure data show that the conformation of the *HPQ* domain is essentially the same when *cyclic CHPQGPPC* and linear *SAWSHPQFEK* bind to streptavidin.[8−10] We further conjugated Aoa-peptides to bovine serum albumin (BSA) so that the peptide−linker−BSA complexes could be immobilized on an epoxy-functionalized glass slide through BSA.[12] The details of the synthesis and conjugation are described in the Appendix. Based on mass spectrometry analysis, we have determined that there are on average three peptides conjugated to one BSA molecule. When a peptide−BSA conjugate is immobilized on an epoxy-coated glass surface, different local environments where the three conjugated peptides are situated on BSA modify binding kinetics when the peptides are subsequently reacted with a protein probe. This modification is taken into consideration in the analysis of the association−dissociation curves.

Preparation of Target Microarrays and Procedure of Subsequent Reactions. For streptavidin−peptide reactions, we printed duplicates of a titration series of the two peptide−BSA complexes (dissolved in 1× PBS solution) on an epoxy-coated glass slide at eight concentrations increasing from 0.7 to 91 μM. In addition, we also printed biotin-conjugated BSA and unmodified BSA as control spots. The printing was done with an OmniGrid100 contact-printing arrayer (Genomic Solutions, Ann Arbor, MI). The printed glass slide was allowed to dry for at least 1 day before immersion in 1× PBS overnight to wash off excess targets and buffer materials. The washed slide was then assembled into a custom-made flow cell with optical access and was washed twice again with a flow of 1× PBS at a rate of 30 mL/min. Afterward, the glass slide was blocked with BSA (7.6 μM in 1× PBS, Jackson ImmunoResearch Laboratories) for 10 min and then washed with fresh 1× PBS for 5 min. The slide was subsequently reacted with streptavidin in 1× PBS: we first filled the flow cell with the streptavidin solution quickly at a rate of 30 mL/min and then slowed down the flow rate to 0.05 mL/min during the observation of the association reaction. Experimentally, we determined that for the fluidic cell used in the present experiment the flow rate of 0.05 mL/min is a factor of 2 larger than the rate beyond which the association−dissociation curves do not change. To observe the dissolution reaction, we first quickly replaced the

(7) Xu, Q.; Miyamoto, S.; Lam, K. S. *Mol. Diversity* **2004**, *8*, 301–310.
(8) Weber, P. C.; Pantoliano, M. W.; Thompson, L. D. *Biochemistry* **1992**, *31*, 9350–9354.
(9) Schmidt, T.; Koepke, J.; Frank, R.; Skerra, A. *J. Mol. Biol.* **1996**, *255*, 753–766.
(10) Katz, B. A. *Biochemistry* **1995**, *34*, 15421–15429.
(11) Giebel, L. B.; Cass, R. T.; Milligan, D. L.; Young, D. C.; Arze, R.; Johnson, C. R. *Biochemistry* **1995**, *34*, 15430–15435.

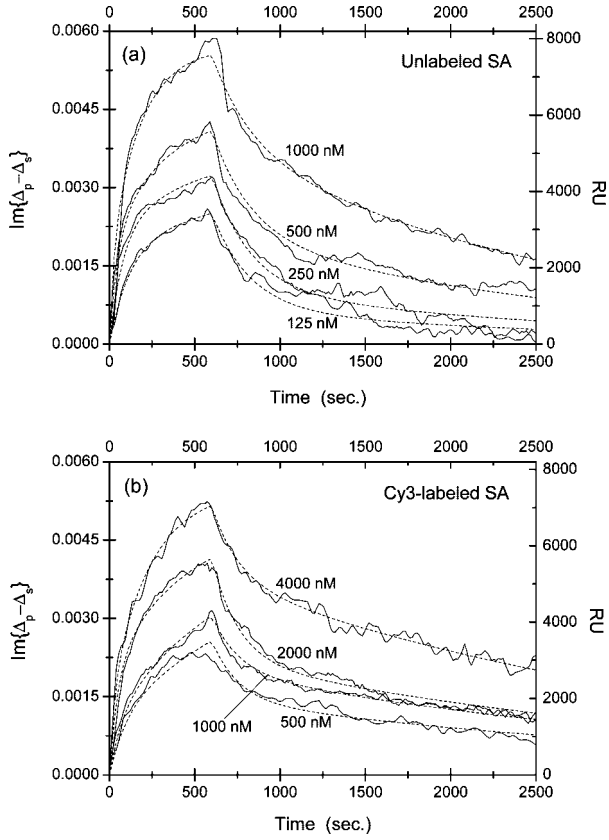

Figure 4. Association−dissociation curves of (a) unlabeled and (b) Cy3-labeled streptavidin with surface-immobilized disulfide-bridged *cyclic CHPQGPPC*−BSA conjugates at different streptavidin concentrations. It should be noted that the probe concentrations in (b) are 4 times larger than those in (a). The dotted lines are global fits to a two-site Langmuir reaction model (see main text for details) with the global fitting parameters listed in Table 2.

protein solution with 1× PBS at a flow rate of 30 mL/min and then slowed down the flow rate to 0.05 mL/min during the subsequent dissociation. We monitored the optical signals from all 32 target spots, 8 control spots, and 8 spots in unprinted regions for reference during the reaction so that we obtained 48 real-time curves in one experiment.

For antibody−antigen reactions, we printed duplicates of a titration series of rabbit antibody (dissolved in 1× PBS) as antigen targets on epoxy-coated glass slides at five concentrations increasing from 0.46 to 7.3 μM. In addition, we printed unmodified BSA as control spots. The postprinting processing of the glass slide was the same as that for the peptide-bearing microarray slide. The antigen-bearing slide was reacted with polyvalent or monovalent goat anti-rabbit antibody. We were able to regenerate the reacted antigen slide by flowing 50 mM of glycine at pH = 1 over the microarray-bearing surface for 5 min and then washing with fresh 1× PBS for 5 min. We monitored the optical signals from all 10 target spots, 2 control spots, and 4 spots in the unprinted region as references so that we obtained 16 real-time curves in one experiment.

Optical Scanning Microscope for Label-Free Detection of Protein−Ligand Reactions. In Figure 1, we show the arrangement of an optical scanning microscope. We use a He−Ne laser at wavelength $\lambda = 633$ nm for illumination to avoid the photobleaching of Cy3-labeled protein molecules. Let $r_{p0} = |r_{p0}| \exp(i\Phi_{p0})$ and $r_{s0} = |r_{s0}| \exp(i\Phi_{s0})$ be the respective reflectivity for p- and s-polarized light from a "bare" solid substrate surface. Let $r_p = |r_p| \exp(i\Phi_p)$ and $r_s = |r_s| \exp(i\Phi_s)$ be the reflectivity when a layer of molecules is added to the solid surface or when the surface of the solid substrate is modified (e.g., conformational change of a pre-existing molecular layer) as a result of the biochemical event. The fractional change in reflectivity is given by $\Delta_p = (r_p - r_{p0})/r_{p0}$ and $\Delta_s = (r_s - r_{s0})/r_{s0}$ for the two polarizations. In our scanning optical microscope, we measure the complex $\Delta_p - \Delta_s$ (oblique-incidence reflectivity difference (OI-RD) signal) as the contrast.[13−17] The information on the newly added surface-bound molecular layer is related to $\Delta_p - \Delta_s$ by[13,15,18]

$$\Delta_p - \Delta_s \cong -i\left[\frac{4\pi\varepsilon_s(\tan\phi_{inc})^2\cos\phi_{inc}}{\varepsilon_0^{1/2}(\varepsilon_s-\varepsilon_0)(\varepsilon_s/\varepsilon_0-(\tan\phi_{inc})^2)}\right]\times \frac{(\varepsilon_d-\varepsilon_s)(\varepsilon_d-\varepsilon_0)\Theta}{\varepsilon_d}\left(\frac{d}{\lambda}\right) \quad (1)$$

ϕ_{inc} is the incidence angle. ε_0, ε_d, and ε_s are the optical dielectric constants of the ambient, the surface-bound molecular layer, and the substrate, respectively. d is the thickness of the molecular layer. Θ is the coverage of the layer, defined as the ratio of the surface area covered by the molecular layer to the total available surface area. Changes in mass density, chemical composition, and conformation are reflected by the corresponding changes in ε_d. When the solid substrate, the aqueous ambient, and the surface-bound molecular layer are transparent to the illumination light beam so that ε_0, ε_s, and ε_d are real numbers, only $\mathrm{Im}\{\Delta_p - \Delta_s\}$ is nonzero,

$$\mathrm{Im}\{\Delta_p - \Delta_s\} = -\left[\frac{4\pi\varepsilon_s(\tan\phi_{inc})^2\cos\phi_{inc}}{\varepsilon_0^{1/2}(\varepsilon_s-\varepsilon_0)(\varepsilon_s/\varepsilon_0-(\tan\phi_{inc})^2)}\right]\times \frac{(\varepsilon_d-\varepsilon_s)(\varepsilon_d-\varepsilon_0)\Theta}{\varepsilon_d}\left(\frac{d}{\lambda}\right) \quad (2)$$

We only monitor $\mathrm{Im}\{\Delta_p - \Delta_s\}$ when detecting the binding reactions of proteins with molecular target microarrays. It is noteworthy that up to an incidence-angle-dependent factor, $\Delta_p - \Delta_s$ is proportional to the corresponding surface plasmon resonance (SPR) angle shift, $\delta\theta_{SPR} \approx (3\pi d/\lambda)(\varepsilon_d - \varepsilon_0)/\varepsilon_d$[19,20] when a molecular film of thickness d and optical dielectric constant ε_d are sandwiched between a gold substrate and an aqueous ambient with optical constant ε_0.

The procedures for obtaining $\Delta_p - \Delta_s$ have been described in detail by Thomas and co-workers[13] and thus will not be repeated here. In the present study (see Figure 1), we use a 60° prism and index-matching fluid to form a good optical contact with one side of a glass slide. The other side of the slide is covered with a target microarray and is in contact with an aqueous solution. The illumination beam with a diameter of 10 mm enters one side of the prism and is focused (with a cylindrical lens) to a 15 μm × 10 mm line on the microarray-bearing surface along the y-axis and then totally reflected from the surface. The reflected beam from a 15 μm × 3 mm line segment in the center of the illuminated region exits the other side of the prism. With a 10× objective, the beam is imaged onto a 50 mm long 152-element photodiode detector so that each photodiode detects the light from a 20 μm segment of the illuminated line. We acquire an image of the target microarray by interrogating 152 photodiode elements sequentially for y-scan and mechanically moving the sample stage along the x-axis for x-scan. The pixel dimension is 20 μm × 20 μm.

To acquire real-time binding (association−dissociation) curves from surface-immobilized targets, we select one pixel from each of the printed targets and one pixel from the unprinted region adjacent

(12) Schena, M. *Microarray Analysis*; John Wiley and Sons: Hoboken, NJ, 2003; p 50.
(13) Thomas, P.; Nabighian, E.; Bartelt, M. C.; Fong, C. Y.; Zhu, X. D. *Appl. Phys. A: Mater. Sci. Process.* **2004**, *79*, 131–137.
(14) Landry, J. P.; Zhu, X. D.; Gregg, J. P. *Opt. Lett.* **2004**, *29*, 581–583.
(15) Fei, Y. Y.; Landry, J. P.; Sun, Y. S.; Zhu, X. D.; Luo, J. T.; Wang, X. B.; Lam, K. S. *Rev. Sci. Instrum.* **2008**, *79*, 013708-1–7.
(16) Zhu, X. D.; Landry, J. P.; Sun, Y. S.; Gregg, J. P.; Lam, K. S.; Guo, X. W. *Appl. Opt.* **2007**, *46*, 1890–1895.
(17) Landry, J. P.; Sun, Y. S.; Zhu, X. D. *Appl. Opt.* **2008**, *47*, 3275–3288.
(18) Zhu, X. D. *Phys Rev. B.* **2004**, *69*, 115407-1–5.
(19) Liedberg, B.; Nylander, C.; Lundstrom, I. *Sens. Actuators* **1983**, *4*, 299–304.
(20) Zhu, X. D. *Opt. Commun.* **2006**, *259*, 751–753.

Table 1. Equilibrium Dissociation Constant $K_D = k_{off}/k_{on}$ of Unlabeled and Cy3-Labeled Streptavidin with *Linear* Peptide *SAWSHPQFEK*−Linker−BSA Conjugates[a]

	$\theta^{(1)}$	$k_{on}^{(1)}$ (M^{-1} s^{-1})	$k_{off}^{(1)}$ (s^{-1})	$K_D^{(1)}$ (nM)	$\theta^{(2)}$	$k_{on}^{(2)}$ (M^{-1} s^{-1})	$k_{off}^{(2)}$ (s^{-1})	$K_D^{(2)}$ (nM)
unlabeled streptavidin	0.71	1.7×10^3	1.6×10^{-4}	92 ± 10	0.29	3.3×10^4	6.4×10^{-3}	192 ± 8
Cy3-labeled streptavidin	0.81	1.5×10^3	3.8×10^{-4}	259 ± 12	0.19	8.3×10^3	6.1×10^{-3}	720 ± 74

[a] The conjugates are immobilized on an epoxy-functionalized glass surface through primary amine groups on the BSA surface.

Table 2. Equilibrium Dissociation Constant $K_D = k_{off}/k_{on}$ of Unlabeled and Cy3-Labeled Streptavidin with Disulfide-Bridged *Cyclic* Peptide *CHPQGPPC*−Linker−BSA Conjugates

	$\theta^{(1)}$	$k_{on}^{(1)}$ (M^{-1} s^{-1})	$k_{off}^{(1)}$ (s^{-1})	$K_D^{(1)}$ (nM)	$\theta^{(2)}$	$k_{on}^{(2)}$ (M^{-1} s^{-1})	$k_{off}^{(2)}$ (s^{-1})	$K_D^{(2)}$ (nM)
unlabeled streptavidin	0.55	1.33×10^3	1.44×10^{-4}	108 ± 38	0.45	2.34×10^4	3.0×10^{-3}	130 ± 13
Cy3-labeled streptavidin	0.74	1.0×10^3	3.7×10^{-4}	373 ± 28	0.26	9.2×10^3	7.8×10^{-3}	850 ± 77

to the target as the reference and measure the OI-RD signals from these selected pixels at a fixed time interval smaller than the time constants of the reactions. We take the difference between the OI-RD signal from the target pixel and the OI-RD signal from the neighboring reference pixel to remove the drift in the optical detection system.

3. Results and Discussion: Binding Affinities of Protein to Ligands

We investigated a number of protein−ligand reactions in order to compare the binding kinetics of the unlabeled protein with those of the Cy3-labeled proteins.

Streptavidin−Peptide Reaction. In Figure 2a, we show the association−dissociation curves for reactions of Cy3-labeled and unlabeled streptavidin with surface-immobilized *linear* peptide *SAWSHPQFEK*−BSA conjugates. The curves are obtained by subtracting the curves for the control spots in the unprinted region from the curves for the printed peptide target spots to remove the drift in the detection system. At $t = 0$, the aqueous ambient in contact with the target microarray is quickly changed from 1× PBS to a streptavidin solution at $[c]_{streptavidin} = 1\ \mu M$ (also in 1× PBS.) The kinks in the curves mark the moment when the ambient is restored back to 1× PBS and the captured streptavidin begins to dissociate from the surface-immobilized peptides. The OI-RD signal is also converted to the resonance unit (RU) typically used in surface plasmon resonance sensorgram measurements. The curve for a printed BSA control spot is also shown in Figure 2a. It showed no evidence of nonspecific reaction between the immobilized BSA and liquid-phase streptavidin at a concentration of 1000 nM. In Figure 2b, we show the association−dissociation curves for reaction of streptavidin with surface-immobilized *cyclic* peptide *CHPQGPPC*−BSA conjugates. The *HPQ* sequences on both peptides are expected to bind to the biotin-binding pocket on streptavidin.[8−10] The association−dissociation curves from the duplicates in the same experiment are very similar.

From Figure 2, it is clear that affinities of streptavidin to two peptides are significantly changed when the streptavidin is labeled with Cy3 fluorescent molecules, presumably from a conformational change in the vicinity of the biotin-binding pocket. To quantify the change in affinity, we measured the association and dissociation curves for streptavidin to the two peptides as functions of protein concentration. The results are displayed in Figure 3 for reactions with *linear* peptide *SAWSHPQFEK*, and in Figure 4 for reactions with *cyclic* peptide *CHPQGPPC*.

We can see that the concentration of the Cy3-labeled streptavidin solution needs to be 4 times as high as that of the unlabeled streptavidin solution in order to arrive at the same equilibrium surface concentration of streptavidin−peptide complexes, indicating that the affinity is reduced as a result of Cy3 labeling. Quantitatively, we fit the association−dissociation curves to the Langmuir reaction kinetics.[21−25] In this model, the association rate is assumed to be proportional to the protein concentration $k_{on}[c]$ and the dissociation rate k_{off} is independent of the protein concentration. The equilibrium dissociation constant of a reaction is given by $K_D = k_{off}/k_{on}$. We first attempted to fit the binding curves to a one-site Langmuir reaction kinetic model that assumes one type of surface-immobilized target and one type of liquid-phase probe. The model failed grossly to describe the association−dissociation curves. As we have alluded in the Materials and Methods section, this is not surprising, since peptide targets on immobilized BSA are better characterized as multiple binding sites for streptavidin due to different local environments where peptides are conjugated on BSA and to the variation of the BSA orientation on the glass surface.[23−25] In other words, same peptides but conjugated at different locations on a surface-immobilized BSA molecule are effectively different epitopes for streptavidin probes, and thus, the latter is expected to have different binding affinities to these differently situated peptides. We have chosen to use a two-site Langmuir reaction kinetic model to analyze association−dissociation curves for streptavidin reactions with *HPQ*-containing peptides. The model is sufficient to describe the binding kinetics involving more than one target site on the solid support. In our present study, models with more than two sites involve too many parameters that more than one set of parameters would fit the data.

In the two-site model, let N_1 and $N_1^{(0)}$ be the reacted and initially available numbers of type-1 targets, and N_2 and $N_2^{(0)}$ be the reacted and available numbers of type-2 targets. The total number of the reacted targets during the association reaction is then given by

$$N(t) = \frac{N_1^{(0)} k_{on}^{(1)}[c]}{k_{on}^{(1)}[c] + k_{off}^{(1)}}\left(1 - \exp\left(-\left(k_{on}^{(1)}[c] + k_{off}^{(1)}\right)t\right)\right) + \frac{N_2^{(0)} k_{on}^{(2)}[c]}{k_{on}^{(2)}[c] + k_{off}^{(2)}}\left(1 - \exp\left(-\left(k_{on}^{(2)}[c] + k_{off}^{(2)}\right)t\right)\right) \quad (3)$$

After a time t_0, the protein probe solution is quickly replaced with 1× PBS. Subsequently, the total number of the reacted targets decreases as

(21) Langmuir, I. *J. Am. Chem. Soc.* **1916**, *38*, 2221–2295.
(22) Atkins. P. W. *Physical Chemistry*; W.H. Freeman and Company: San Francisco, 1978; pp 942−944.
(23) Morton, T. A.; Myszka, D. G.; Chaiken, I. M. *Anal. Biochem.* **1995**, *227*, 176–185.
(24) Heding, A.; Gill, R.; Ogawa, Y.; Meyts, P. D.; Shymko, R. M. *J. Biol. Chem.* **1996**, *271*, 13948–13952.
(25) House-Pompeo, K.; Boles, J. O.; Höök, M. *Methods* **1994**, *6*, 134–142.

$$N(t) = \frac{N_1^{(0)} k_{on}^{(1)}[c]}{k_{on}^{(1)}[c] + k_{off}^{(1)}}\left(1 - \exp\left(-\left(k_{on}^{(1)}[c] + k_{off}^{(1)}\right)t_0\right)\right) \times \exp\left(-k_{off}^{(1)}(t - t_0)\right) + \frac{N_2^{(0)} k_{on}^{(2)}[c]}{k_{on}^{(2)}[c] + k_{off}^{(2)}}\left(1 - \exp\left(-\left(k_{on}^{(2)}[c] + k_{off}^{(2)}\right)t_0\right)\right)\exp\left(-k_{off}^{(2)}(t - t_0)\right) \quad (4a)$$

The surface coverage of streptavidin-peptide complexes $\Theta_{streptavidin}$ is proportional to $N(t)$,

$$\Theta_{streptavidin} \propto N(t) \quad (4b)$$

From eq 2, the optical signals shown in Figures 2−4 are expected to vary as

$$\mathrm{Im}\{\Delta_p - \Delta_s\} \sim \frac{N_1^{(0)} k_{on}^{(1)}[c]}{k_{on}^{(1)}[c] + k_{off}^{(1)}}\left(1 - \exp\left(-\left(k_{on}^{(1)}[c] + k_{off}^{(1)}\right)t\right)\right) + \frac{N_2^{(0)} k_{on}^{(2)}[c]}{k_{on}^{(2)}[c] + k_{off}^{(2)}}\left(1 - \exp\left(-\left(k_{on}^{(2)}[c] + k_{off}^{(2)}\right)t\right)\right) \quad (5)$$

for $0 < t < t_0$, and

$$\mathrm{Im}\{\Delta_p - \Delta_s\} \sim \frac{N_1^{(0)} k_{on}^{(1)}[c]}{k_{on}^{(1)}[c] + k_{off}^{(1)}}\left(1 - \exp\left(-\left(k_{on}^{(1)}[c] + k_{off}^{(1)}\right)t_0\right)\right) \times \exp\left(-k_{off}^{(1)}(t - t_0)\right) + \frac{N_2^{(0)} k_{on}^{(2)}[c]}{k_{on}^{(2)}[c] + k_{off}^{(2)}}\left(1 - \exp\left(-\left(k_{on}^{(2)}[c] + k_{off}^{(2)}\right)t_0\right)\right)\exp\left(-k_{off}^{(2)}(t - t_0)\right) \quad (6)$$

for $t > t_0$.

For each set of association−dissociation curves in Figures 3 and 4, we performed a global fitting using eqs 5 and 6 with $k_{on}^{(1)}$, $k_{off}^{(1)}$, $k_{on}^{(2)}$, $k_{off}^{(2)}$, $N_1^{(0)}/(N_1^{(0)} + N_2^{(0)}) \equiv \theta^{(1)}$, and $N_2^{(0)}/(N_1^{(0)} + N_2^{(0)}) \equiv \theta^{(2)}$ as global fitting parameters. The dotted lines in these figures are the fits to the model. In Table 1, we list the kinetic constants and other parameters for streptavidin reactions with *linear* peptide *SAWSHPQFEK*−BSA conjugates. In Table 2, we list the kinetic constants and other parameters for streptavidin reactions with disulfide-bridged *cyclic* peptide *CHPQGPPC*−BSA conjugates. The fitting parameters from duplicate target spots are the same within the error bars. In our present experiment, averaging the curves from repeat spots improves the signal-to-noise ratio only slightly.

For streptavidin reaction with *linear SAWSHPQFEK*, when streptavidin is Cy3-labeled, the dissociation constant K_D increases by a factor of 3 at the majority site, and mostly k_{off} becomes larger due to labeling. At the minority site, the dissociation constant K_D increases by a factor of 4, and in this case k_{on} becomes smaller due to labeling.

For streptavidin reaction with disulfide-bridged *cyclic CHPQGPPC*, when streptavidin is Cy3-labeled, the dissociation constant K_D increases by a factor of 4 at the majority site, again because k_{off} becomes larger. At the minority site, the dissociation constant K_D increases by a factor of 7, in this case as a result of a combination of a decrease in k_{on} by a factor of 2.5 and an increase in k_{off} by a factor of 2.5.

Antibody−Antigen Reaction. In Figure 5, we show the association−dissociation curves for reaction of monovalent F_{ab} fragment of goat IgG against the (H+L) domain of rabbit IgG with the surface-immobilized rabbit IgG. From the appearance of the curves, we might conclude that the Cy3-labeling had little effect on the affinity. However, when we analyze the association−dissociation curves consistently with the two-site Langmuir model, we find the conclusion is more complex and worthy of further elaboration. We note here that the one-site Langmuir model does not fit the experimental observation very well. In this case, the multiplicity of antigen targets comes primarily from different orientations at which the targets are immobilized when reacting with epoxy groups on the glass surface. As a result, we need to resort to the two-site Langmuir reaction model to better describe the characteristics of the target population on the solid support. As shown by dotted lines, we performed the global fitting using eqs 5 and 6 to the association−dissociation curves in Figure 5 with $k_{on}^{(1)}$, $k_{off}^{(1)}$, $k_{on}^{(2)}$, $k_{off}^{(2)}$, $N_1^{(0)}/(N_1^{(0)} + N_2^{(0)}) \equiv \theta^{(1)}$, and $N_2^{(0)}/(N_1^{(0)} + N_2^{(0)}) \equiv \theta^{(2)}$ as fitting parameters. The parameters are tabulated in Table 3.

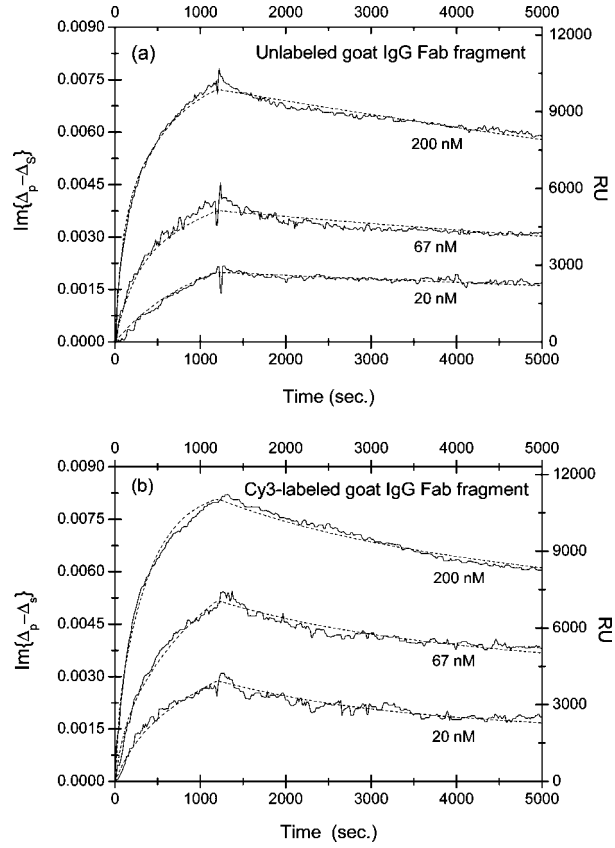

Figure 5. Association−dissociation curves of (a) unlabeled and (b) Cy3-labeled monovalent F_{ab} fragment of goat IgG against the (H+L) domain of rabbit IgG with surface-immobilized rabbit IgG at different goat IgG concentrations. The curves are globally fitted (dotted lines) to a two-site Langmuir reaction model (see main text for details) with the global fitting parameters listed in Table 3.

The equilibrium dissociation constant for the monovalent F_{ab} fragment of goat IgG with the surface-immobilized rabbit IgG at the majority sites (type-2) decreases by a factor of 3 due to Cy3- labeling, due to a combination of an increase in k_{on} by a factor of 1.5 and a decrease in k_{off} by a factor of 2. In contrast, the equilibrium dissociation constant for the same reaction with rabbit IgG at the minority sites (type-1) increases instead by a factor of 4 due to labeling, in this case as a result of a significant increase in the dissociation rate k_{off}.

In Figure 6, we show the association−dissociation curves for reactions of unlabeled and Cy3-labeled goat whole antibodies (against the F_c fragment of rabbit IgG) with surface-immobilized rabbit IgG. The dotted lines are the result of a global fitting using eqs 5 and 6 with $k_{on}^{(1)}$, $k_{off}^{(1)}$, $k_{on}^{(2)}$, $k_{off}^{(2)}$, $N_1^{(0)}/(N_1^{(0)} + N_2^{(0)}) \equiv \theta^{(1)}$, and $N_2^{(0)}/(N_1^{(0)} + N_2^{(0)}) \equiv \theta^{(2)}$ as the fitting parameters. The fitting parameters are tabulated in Table 4.

Table 3. Equilibrium Dissociation Constant $K_D = k_{off}/k_{on}$ of Reaction of Unlabeled and Cy3-Labeled Monovalent F_{ab} Fragments of Goat IgG (against the (H+L) Domain of Rabbit IgG) with Surface-Immobilized Rabbit IgG Targets

	$\theta^{(1)}$	$k_{on}^{(1)}$ (M^{-1} s^{-1})	$k_{off}^{(1)}$ (s^{-1})	$K_D^{(1)}$ (nM)	$\theta^{(2)}$	$k_{on}^{(2)}$ (M^{-1} s^{-1})	$k_{off}^{(2)}$ (s^{-1})	$K_D^{(2)}$ (nM)
unlabeled goat IgG	0.38	6.8×10^4	5.3×10^{-5}	0.78 ± 0.12	0.62	0.78×10^4	6.3×10^{-5}	8.0 ± 1.2
Cy3-labeled goat IgG	0.17	1.6×10^5	5.2×10^{-4}	3.4 ± 0.4	0.83	1.3×10^4	3.1×10^{-5}	2.40 ± 0.16

Table 4. Equilibrium Dissociation Constant $K_D = k_{off}/k_{on}$ of Reaction of Unlabeled and Cy3-Labeled Goat Whole IgG (against the F_c Domain of Rabbit IgG) with Surface-Immobilized Rabbit Igg Targets

	$\theta^{(1)}$	$k_{on}^{(1)}$ (M^{-1} s^{-1})	$k_{off}^{(1)}$ (s^{-1})	$K_D^{(1)}$ (nM)	$\theta^{(2)}$	$k_{on}^{(2)}$ (M^{-1} s^{-1})	$k_{off}^{(2)}$ (s^{-1})	$K_D^{(2)}$ (nM)
unlabeled goat IgG	0.33	3.6×10^4	2.5×10^{-5}	0.70 ± 0.13	0.67	2.4×10^3	3.2×10^{-5}	13.6 ± 1.9
Cy3-labeled goat IgG	0.22	4.1×10^4	1.3×10^{-4}	3.20 ± 0.44	0.78	2.5×10^3	6.9×10^{-6}	2.81 ± 0.22

Similarly, the equilibrium dissociation constants for the whole goat IgG with the surface-immobilized rabbit IgG at the majority site (type-2) decreases by a factor of 5 as a result of Cy3-labeling, primarily from a decrease in dissociation rate k_{off}. In contrast, the equilibrium dissociation constant for the same reaction with the rabbit IgG at the minority site (type-1) increases by a factor of 5 as a result of labeling, mostly from an increase in dissociation rate k_{off} (by a factor of 5).

Discussion. Using titration calorimetric (label-free detection) methods, Weber and co-workers reported binding kinetic measurements on other streptavidin−linear peptide pairs and found $K_D = 126$ μM for streptavidin−*FSHPQNT* reaction and $K_D = 282$ μM for streptavidin−*HDHPQNL* reaction.[8] Our measurement of streptavidin−*SAWAHPQFEK* reaction with the peptide target immobilized on a solid support yields K_D that is 3 orders of magnitude smaller. It is unclear and in fact worthy of investigation whether the difference here has to do with different methods or different linear peptides. Using the surface plasmon resonance method (another label-free detection technique for studying surface-immobilized targets), Giebel and co-workers measured the association−dissociation curves for a number of cyclic HPQ-containing peptides.[11] For streptavidin−*AECHPQGPPCIEGRK* reaction, these authors reported $K_D = 230$ nM. Our measurement of $K_D \sim 120$ nM for streptavidin−*CHPQGPPC* is a factor of 2 smaller. It seems that the two surface-immobilization-based methods yield comparable K_D values for the same reactions. However, we should point out that the binding curves reported by Giebel et al.[11] were unusually deviant from Langmuir kinetics, even for a two-site model, and thus, the numerical meaning of their reported $K_D = 230$ nM for streptavidin−*AECHPQGPPCIEGRK* reaction is not without question. To the best of our knowledge, there are no prior reports of K_D for the antibody−antigen binding reactions that we investigated in the present work.

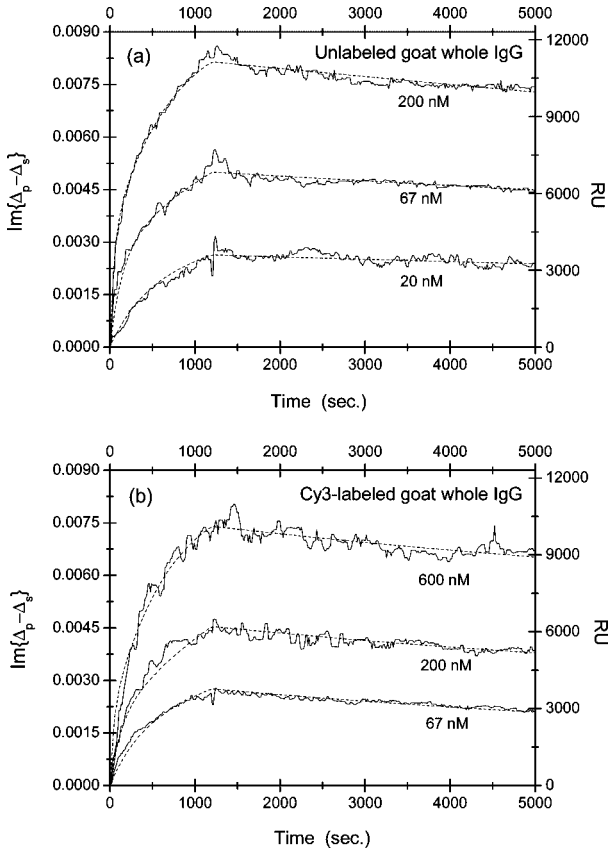

Figure 6. Association−dissociation curves of (a) unlabeled and (b) Cy3-labeled goat anti-rabbit whole IgG against the F_c domain of rabbit IgG with surface-immobilized rabbit IgG at different goat IgG concentrations. The dotted lines are global fits to a two-site Langmuir reaction model (see main text for details) with the global fitting parameters listed in Table 4.

We now discuss the significance of Figures 2−6 and particularly the extracted affinity parameters in Tables 1−4. For streptavidin−peptide interaction, X-ray crystallographic studies by Weber et al.[8] and Katz[10] established that the HPQ sequence on a peptide forms direct and indirect (through a water molecule) hydrogen bonds with Serine-27, Serine-43, Serine-88, Threonine-90, and Asparte-128 on streptavidin. Conjugation of Cy3 molecules takes place at Lysine-80, Lysine-121, Lysine-132, and Lysine-134 on a monomeric streptavidin and thus does not directly block the peptide binding site. However, the close proximity of all four lysine residuals to Serine-88, Threonine-90, and Asparte-128 makes Cy3-conjugation at these residuals susceptible to local conformational changes that can affect either the access (k_{on}) or the binding energy (k_{off}) of the HPQ-containing peptide ligand to the binding site. Since the Cy3-to-streptavidin ratio is 2.5−3.5, on average every monomeric unit on a streptavidin tetramer is conjugated with one Cy3 dye molecule. As a result, it is not surprising if the Cy3-labeled streptavidin exhibits qualitatively different binding kinetics when reacting with HPQ-containing peptides. This is what we observed. Independent of the Langmuir reaction model, it is clear from our data that the affinity of streptavidin to two HPQ-containing peptides is significantly lowered by having streptavidin labeled with Cy3 dye. Using the two-site Langmuir kinetics model, we can quantify the change in more detail. For the majority of the *linear* peptide *SAWSHPQFEK* on the glass surface (type-1), the Cy3-labeled streptavidin has the same access to the HPQ motif (evident from similar association rate constant k_{on}) but forms a less stable complex (implicated by a larger dissociation rate k_{off}). This suggests that there is a conformational change in the Cy3-labeled streptavidin leading to the formation of a less stable streptavidin−HPQ complex. For the minority of the peptide on the glass surface (type-2), the Cy3-labeled streptavidin has a somewhat hindered access to the HPQ motif (as suggested by a smaller association constant k_{on}) though afterward forming an

equally stable complex with the motif. The stereohindrance for the Cy3-labeled streptavidin to reach the HPQ motif may have contributed to the stability of the resultant complex. Similarly, for the majority of the disulfide-bridged *cyclic* peptide *CHPQG-PPC* on the glass surface (type-1), the Cy3-labeled streptavidin forms a less stable complex with the HPQ motif as implicated by a larger dissociation rate k_{off}. Again, we attribute it to a conformational change in the labeled streptavidin that bears a direct consequence on the stability of the streptavidin−HPQ complex. For a minority of the disulfide-bridged *cyclic* peptide *CHPQGPPC* on the glass surface (type-2), again the reduced association rate constant for the Cy3-labeled streptavidin suggests a hindered access to the HPQ motif as a result of labeling. In this case, the stereohindrance to the labeled streptavidin has not helped to stabilize the streptavidin−HPQ complex as it did for the linear peptide *SAWSHPQFE* at the minority site. The stereohindrance for the Cy3-labeling streptavidin to access the minority peptides on the glass surface stems either directly from the added Cy3 molecule or through the labeling-induced conformational change. A temperature dependence study (beyond the scope of the present work) will help to determine whether the conformational change is predominant, as it should exhibit strong temperature dependence. We note here that having multiple binding sites for a streptavidin molecule due to differently situated peptides on a surface-bound BSA does not necessarily increase the likelihood that the fluorescent labels interfere with the affinity of the host molecule to the sites. It simply changes how the fluorescent labels interfere with the affinity of the host molecule to these sites.

The Cy3-labeling effect on antibody−antigen binding reactions is subtle. Since there are 72 lysine residuals on a single IgG molecule, 38 in the F_c domain and 17 in each of the two monovalent F_{ab} fragments, even though some of them may not be available for conjugation, having 3 out of 17 lysine residuals on a monovalent F_{ab} fragment and 5 out of 38 lysine residuals on the F_c domain conjugated with Cy3 molecules may not have a direct blocking effect or a close proximity effect on antibody−antigen binding reaction as on the aforementioned streptavidin−peptide interaction. Without a quantitative analysis based on a two-site Langmuir reaction model, the affinities of the whole goat antibody and the monovalent F_{ab} fragment against rabbit IgG do not seem to change significantly. However, when subjected to the analysis using Langmuir reaction kinetic models, we find that the association and dissociation curves are not fit well with the Langmuir reaction kinetics with one type of immobilized target on a glass surface. Instead, they are fit much better with a Langmuir reaction kinetic model that assumes two types of immobilized targets on the glass surface. Within such a two-site reaction kinetic model, we arrive at the conclusion that Cy3-labeling of a goat whole antibody or its F_{ab} fragment can increase or decrease the affinity of the antibody to the antigen target. Depending on the local configuration of the epitope and the corresponding environment, the Cy3-labeled antibody may form either a more stable or less stable complex with the target as is evident from Tables 3 and 4.

4. Concluding Remarks

Fluorescently labeling a protein can significantly change the affinity of the protein with ligands and alter the equilibrium concentrations of protein−ligand complexes that can be consequential. In cases when a binding site for a ligand to a protein is not directly blocked by conjugation of fluorescent tags to the protein, the local conformational change of the protein, particularly when the conjugation sites are in close proximity to the ligand binding site, and the protein−ligand binding kinetics can still be altered profoundly. Label-free detection of protein−ligand and glycan−ligand reactions, though not yet as sensitive as fluorescence-based detection, is desirable and useful even just for quantifying the effect of fluorescent labeling.

Acknowledgment. This work was supported by the National Institutes of Health under R01-HG3827.

Appendix
Preparation of Ketone−BSA Scaffold

A total of 1 mg of BSA was dissolved in 5 mL of 0.1 M $NaHCO_3$. The solution was mixed with 0.5 mL levulinic acid NHS ester solution (50 μmol in 0.5 mL of DMSO) and stirred overnight at room temperature to allow the reaction to complete. The mixture was then adjusted to pH 6.0 and dialyzed against 1 L of double-distilled H_2O and lyophilized to yield ketone−BSA conjugates in the form of white powder. Matrix-assisted laser desorption ionization time-of-flight mass spectrometry (MALDI-TOF MS) analysis showed that on average there are three ketone groups per synthesized ketone−BSA conjugate.

Peptide Synthesis

We synthesized two Aoa-linked peptides, disulfide-bridged *cyclic CHPQGPPC* and linear *SAWSHPQFEK*, by Fmoc chemistry on Linker−linker−K (Aoa−Boc)-preloaded Rink Amide resin, as mentioned above. All couplings were performed using HOBt/DIC as coupling agents in DMF (*N*,*N*′-dimethylformamide). The peptide−linker−linker−Lys(Aoa)−NH_2 products were cleaved from the resin and were purified by reverse phase HPLC. The molecular identities were confirmed by MALDI-TOF MS.

Preparation of Peptide−BSA Conjugates

A total of 0.1 mg of ketone−BSA and 0.1 mg of peptide compound were dissolved in 0.2 mL of 0.05 M sodium acetate buffer (pH 4.5), stirred at room temperature for 5 h, then dialyzed against ddH_2O, and finally lyophilized. The resultant white powder was dissolved in PBS and used for microarray deposition. On average, three peptide molecules are bound to one BSA molecule.[7]

LA802097Z